Monitoring a snowpack's ability to store liquid water at the small catchment scale

Ryan W. Webb*, Center for Water and the Environment, University of New Mexico Keith Musselman, Institute of Arctic and Alpine Research, University of Colorado Boulder Katherine Hale, Geography Department, University of Colorado Boulder Noah Molotch, Geography Department, University of Colorado Boulder

Summary

An important consideration for water resources planning is runoff timing, which can be strongly influenced by the physical process of water storage within and release from seasonal snowpacks. The aim of this presentation is to introduce a novel method that combines light detection and ranging (LiDAR) with ground-penetrating radar (GPR) to nondestructively estimate the spatial distribution of bulk liquid water content in a seasonal snowpack during spring melt. This method was developed at multiple plots in Colorado in 2017 and applied at the small catchment scale in 2019. We developed this method in a manner to observe rapid changes that occur at subdaily timescales. Observed volumetric liquid water contents ranged from near zero to 19%vol within the scale of meters during method development. We also show rapid changes in bulk liquid water content of up to 5%vol that occur over subdaily timescales. The presented methods have an average uncertainty in bulk liquid water content of 1.5%vol, making them applicable for studies to estimate the complex spatiotemporal dynamics of liquid water in snow. During the spring snowmelt season of 2019, we applied this method to a small headwater catchment in the Colorado Front Range. A total of 9 GPR surveys of approximately 3 km in length were conducted over a six-week period. Additionally, five LiDAR scans occurred over the same area. Using this technique, we identify locations that melting snow accumulates and is stored as liquid water within the snowpack. This work shows that the vadose zone may be conceptualized, during snowmelt, as extending above the soil-snow interface to include variably saturated flow processes within the snowpack.

Introduction

For many communities and ecosystems around the globe, valuable water resources originate from snow. In particular, mid-latitude and semi-arid regions, such as the western U.S., rely on snow for much of the annual downstream water supply that is of high economic importance. Thus, it is important to understand the physical processes that occur during snowmelt runoff in mountainous terrain to further determine how a changing climate will alter the availability of water resources. In order to accomplish this further understanding, observations of snowmelt flow paths are necessary.

Appropriately representing snowmelt infiltration at the hillslope scale is important to predicting streamflow. However, infiltration beneath a melting snowpack can be highly variable both temporally and spatially as a result of preferential flow paths. The movement of water along sloping interfaces creates focused infiltration (Webb et al., 2018a) and can deposit water directly into a stream channel, bypassing soil interaction (Eiriksson et al., 2013). The complexity of this process increases as slope and forest canopy effects are introduced (e.g. Webb et al., 2018b), justifying the need to observe the spatial variability of meltwater flow in complex environments.

Continuously observing the liquid water content (LWC) of snow has advanced in recent years for point measurements. One recent method uses upward looking ground penetrating radar (GPR) (Heilig et al., 2015). Spatially observing LWC has also been accomplished using GPR methods over short distances for a single point in time (Bradford et al., 2009). Bradford et al. (2009) non-destructively estimated LWC over a 35 m long transect using 16 passes over the same transect. However, these studies for observing the LWC of snow are limited either spatially to a point or short transect, or temporally to a single point in time. For this study, we combine LiDAR-based measurements of snow depth with observations from a common offset pulse wave GPR system.

The goal of this presentation is to introduce a methodology that combines LiDAR and GPR to non-destructively estimate the spatial distribution of bulk LWC in a seasonal snowpack during spring snowmelt. The work presented

- Introduce the method as it was developed and applied to plot-scale sites in Colorado during the 2017 spring snowmelt season.
- Apply the methodology at the small watershed scale during the 2019 spring snowmelt season to characterize how a snowpack stores liquid water.

Methods

Site Description

This research method was developed at three study plots in the Colorado Rocky Mountains during the snowmelt season of 2017 and applied in one study watershed during spring snowmelt of 2019. The plots span in elevation from the rainsnow transition zone to the high alpine. The study watershed lies within the Niwot Ridge Long Term Ecological Research area, spanning elevations from 3350 to 3500 masl (Fig. 1).



Figure 1: Aerial image of the experimental watershed (approximate watershed delineation in red).

Terrestrial LiDAR

The spatial distribution of snow depth (d_s) was determined using terrestrial LiDAR scanning. We used a Riegl VZ-400 LiDAR scanner that has a manufacturer reported accuracy of 5 mm in ideal conditions. Georeferencing and aligning multiple scans was accomplished using Trimble Business Center and Riegl RiSCAN Pro software packages. Ground surface scans were georeferenced using four 16.5 cm diameter reflective targets with Trimble R10 rover GPS units (minimum of 20-minute occupation time) corrected to a Trimble NetR9 base station with a Zephyr Geodetic antenna. Snow surface scans occurred from as close to the same positions as possible for continuity between scans. We estimate a maximum error of ~5 cm based on ground vegetation height at less than ideal scanning angles, with an average post-processing accuracy of 2 cm for d_s. The LiDAR scans were aggregated to produce 50 cm resolution digital elevation models (DEMs) of the ground and snow surfaces for plot-scale analyses and at 3.0 m resolution for the small watershed scale analysis. Snow depth was then calculated by subtracting the ground surface DEMs from snow surface DEMs. Methods described below were only applied to snow depths greater than 20 cm.

GPR

Two-way-traveltime (TWT) of GPR waves through snow were obtained on the same days as snow surface LiDAR scans. We used a Mala Geoscience, Inc. ProEx control unit pulse GPR system with an 800 MHz shielded antenna. The antenna was fixed in place on a plastic sled towed behind the user. A GPS antenna connected to the ProEx control unit registered location information every second. Radar pulses

were triggered on 0.05 s intervals using eight times stacking and a total time window of 50 ns. The average survey travel speed was ~0.5 m/s resulting in ~40 returns per meter. The ReflexW Software package was used for time-zero adjustment, taken as the first break in the first wavelet, a dewow filter, and background removal. The reflection of the snow-soil interface (e.g. Fig. 2) was then picked at the first break prior to the first peak of the reflection and TWT averaged over 50 cm and 3.0 m increments for the plot-scale and watershed scale analyses, respectively. Surface topography was corrected for by dividing by the cosine of the ground surface slope at that location.

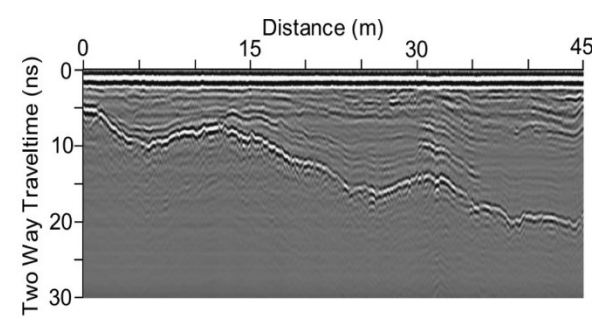


Figure 2: Example radargram displaying the reflection from the snow-soil interface under a melting snowpack.

Estimating Liquid Water Content

The effective dielectric permittivity (ε_{eff}) of snow is sensitive to snowpack density and LWC, and is calculated from the observed velocity (v) of the radar wave through snow (e.g. Mitterer et al., 2011):

$$\varepsilon_{\rm eff} = \left(\frac{c}{v}\right)^2$$
 (Eq. 1)

Where c is the speed of light in a vacuum (~0.3 m/ns) and v is calculated using:

$$v = \frac{d_s}{(TWT/2)}$$
 (Eq. 2)

The bulk volumetric LWC ($\theta_{\rm w}$) of snow is then calculated from $\varepsilon_{\rm eff}$ using the Roth et al. (1990) three phase mixing model that is commonly applied (e.g. Heilig et al., 2015; Mitterer et al., 2011):

$$\theta_{w} = \frac{\epsilon_{eff}^{0.5} - \frac{\rho_{d}}{\rho_{i}} \epsilon_{i}^{0.5} - \left(1 - \frac{\rho_{d}}{\rho_{i}}\right) \epsilon_{a}^{0.5}}{\epsilon_{w}^{0.5} - \epsilon_{o}^{0.5}}$$
(Eq. 3)

Where ρ_d is the dry density of snow, ρ_i is the density of ice (917 kg/m³), ε_i , ε_a , and ε_w are the dielectric permittivities of ice, air, and liquid water, respectively. At 0°C these dielectric permittivities are known ($\varepsilon_i = 3.18$, $\varepsilon_a = 1.0$, and ε_w = 87.9). For this study we observe ρ_d through manual snow pit measurements and assume it is spatially uniform within each plot. For the watershed scale analysis, two snow pits were dug to observe bulk density and used for ρ_d for the associated area of the watershed.

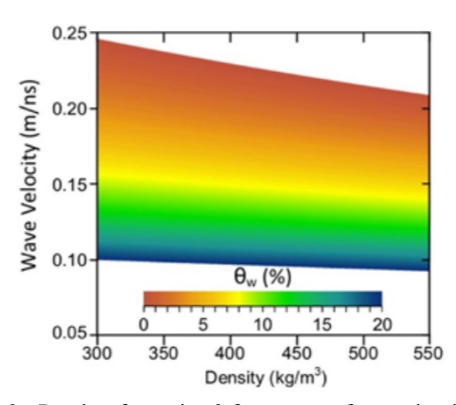


Figure 3: Results of equation 3 for a range of snow dry densities from $300 - 550 \text{ kg/m}^3$ and radar wave velocities from 0.09 - 0.25m/ns. Only volumetric liquid water content (θ_w) values between 0 and 20% are shown (modified from Webb et al. (2018c)).

When Equation 3 is applied to a range of snow densities, it can be seen that the resulting θ_w is more sensitive to the radar wave velocity than the snow density (Fig. 3). These methods result in an average uncertainty in θ_w of 1.5% (Webb et al., 2018c).

Results & Discussion

The developed methods allow for non-destructive observations of the spatial distribution of liquid water in a melting snowpack at spatial scales and time intervals not previously achieved through the combined use of GPR, LiDAR, and snow pit observations. We used this method to observe rapid changes in $\theta_{\rm w}$ of a snowpack at the plot and hillslope scales during method development. Results display the high spatial and temporal variability of θ_w in a seasonal snowpack during melt (Webb et al., 2018c, 2020). Results displayed the high spatial variability that θ_w can have during spring snowmelt and the non-uniform manner that a snowpack stores and transmits liquid water. This is a result of the influence that intra-snowpack flow paths have on the accumulation of LWC at downslope locations (Webb et al., 2020).

When conducting these observations at the small watershed scale, $\theta_{\rm w}$ variability can be observed in large scale patterns during peak melt on June 7, 2019 (Fig. 4). Areas of accumulation occur in the same location as the plot-scale study. However, in the watershed scale observations, we see

that the liquid water storage extends a greater distance at the downslope end of the plot where the convergence of flow paths occurs.

Furthermore, June 7, 2019 had an incoming winter storm that inhibited active snowmelt from occurring that day. Therefore, the locations of observed high θ_w are from previous snowmelt days. Our results indicate that it is important to consider the storage characteristics of the snowpack itself. It is likely that the soil beneath the snowpack is saturated in locations of increased snow liquid water storage observed that creates areas of increased gradients for groundwater recharge and physical flow paths of connectivity both above and below the snow-soil interface that have yet to be represented in hydrological modeling efforts. Layers within a snowpack have hydraulic conductivities that are often orders of magnitude greater than most common soils (Calone et al., 2012) indicating the importance of intra-snowpack flow path considerations for appropriately representing physical processes during snowmelt in hydrological models. Our results here indicate a physical process that contributes to the uncertainty of hydrologic models that has yet to be fully quantified. This work shows that the vadose zone may be conceptualized, during snowmelt, as an extending above the snow-soil interface to include variably saturated flow processes within the snowpack.

Future investigations will examine the changes of liquid water storage in snow through time, including analysis of 9 total GPR surveys over a 6-week period at the small watershed scale example location. The June 7, 2019 data collection shown in Fig. 4 represents the median date of observations. Future analyses will be conducted on the temporal changes prior to, and after these data.

Conclusions

We present a method that allows for the non-destructive observation of the spatial distribution of liquid water in a melting snowpack from the plot to small watershed scale. This work shows that the snowpack may be conceptualized, during snowmelt, as an extension of the vadose zone as variably saturated flow processes occur in both the soil and snow.

Acknowledgements

This work was supported by the National Science Foundation Award number 1824152 and the Niwot Ridge LTER cooperative agreement number DEB-1637686

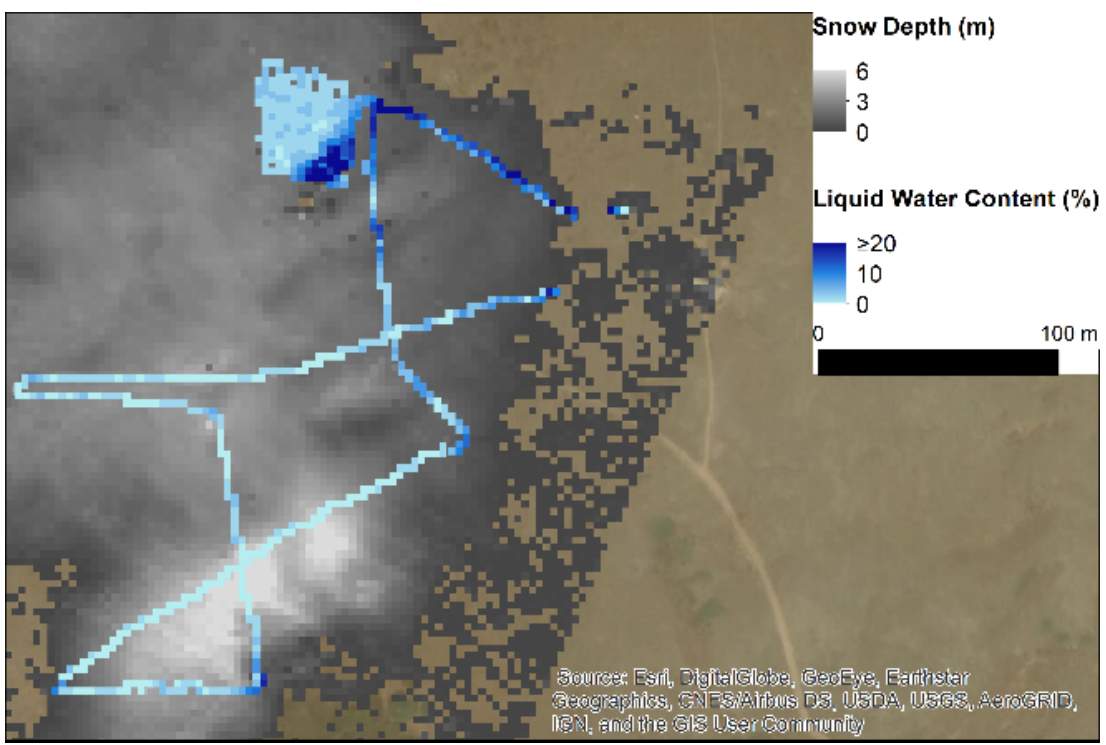


Figure 4: Results of watershed scale observations for June 7, 2019. All data were aggregated to a resolution of 3 m.

References

Bradford, J., J. Harper, and J. Brown (2009). Complex dielectric permittivity measurements from groundpenetrating radar data to estimate snow liquid water content in the pendular regime. Water Resources Research, 45, doi: 10.1029/2008WR007341.

Calonne, N., Geindreau, C., Flin, F., Morin, S., Lesaffre, B., Rolland du Roscoat, S., Charrier, P. (2012). 3-D image-based numerical computations of snow permeability: links to specific surface area, density, and microstructural anisotropy. Cryosphere 6(5), 939-951. doi: 10.5194/tc-6-939-2012

Eiriksson, D., M. Whitson, C. H. Luce, H. P. Marshall, J. Bradford, S. G. Benner, T. Black, H. Hetrick, and J. P. McNamara (2013). An evaluation of the hydrologic relevance of lateral flow in snow at hillslope and catchment scales. Hydrological Processes, 27(5), 640-654, doi: 10.1002/hyp.9666.

Heilig, A., C. Mitterer, L. Schmid, N. Wever, J. Schweizer, H. Marshall, and O. Eisen (2015). Seasonal and diurnal cycles of liquid water in snow-Measurements and modeling. Journal of Geophysical Research-Surface, 120(10), 2139-2154, Earth 10.1002/2015JF003593.Mitterer et al., 2011

Roth, K., R. Schulin, H. Fluhler, and W. Attinger (1990). Calibration of Time Domain Reflectometry for

Water-Content Measurement using a Composite Dielectric Approach. Water Resources Research, 26(10), 2267-2273, doi: 10.1029/WR026i010p02267.

Webb, R. W., M. Williams, and T. Erickson (2018a). The Spatial and Temporal Variability of Meltwater Flowpaths: Insights from a grid of over 100 Snow Lysimeters. Water Resources Research. 54, 1146-1160, doi: 10.1002/2017WR020866.

Webb, R. W., S. R. Fassnacht, M. N. Gooseff, and S. W. Webb (2018b). The Presence of Hydraulic Barriers in Layered Snowpacks: TOUGH2 Simulations and Estimated Diversion Lengths. Transport in Porous Media, 123(3), 457-476, doi: 10.1007/s11242-018-1079-1

Webb, R. W., Jennings, K. S., Fend, M., & Molotch, N. P. (2018c). Combining ground-penetrating radar with terrestrial LiDAR scanning to estimate the spatial distribution of liquid water content in seasonal snowpacks. Water Resources Research, 54, 10,339-10,349. https://doi.org/10.1029/2018WR022680

Webb, RW, Wigmore, O, Jennings, K, Fend, M, Molotch, NP (2020). Hydrologic connectivity at the hillslope scale through intra-snowpack flow paths during snowmelt. Hydrological Processes. https://doi.org/10.1002/hyp.13686